ANALYSIS OF STATIC AND DYNAMIC CHARACTERISTICS OF HUMIDITY SENSORS

Kitano, Masaharu
Biotron Institute Kyushu University

Eguchi, Hiromi
Biotron Institute Kyushu University

Matsui, Tsuyoshi
Biotron Institute Kyushu University

出版情報：BIOTRONICS. 13, pp.11-28, 1984-10. Biotron Institute, Kyushu University
バージョン：
権利関係：

BIOTRONICS **13**, 11–28, 1984

ANALYSIS OF STATIC AND DYNAMIC CHARACTERISTICS OF HUMIDITY SENSORS

Masaharu KITANO, Hiromi EGUCHI and Tsuyoshi MATSUI

Biotron Institute, Kyushu University, Fukuoka 812, Japan

(Received September 6, 1984)

KITANO M., EGUCHI H. and MATSUI T. *Analysis of static and dynamic characteristics of humidity sensors.* BIOTRONICS **13**, 11–28, 1984. For adequate measurement of air humidity in plant environment, characteristics of humidity sensors of ventilated psychrometer of resistance thermometers (Ps), lithium chloride relative humidity sensor (Lr), electric capacitance meter with filter (Ec), electric capacitance meter without filter (Ec-n) and absolute humidity sensor of thermistors (Ab) were examined. Static characteristics indicated that all sensors used can be applied to humidity measurement with sufficient accuracies in steady state. In dynamic characteristics, appreciable differences were found among these sensors; Ec-n was more sensitive to both absolute humidity dynamics and air temperature dynamics as compared with Ps, Lr, Ec and Ab. In particular, Lr and Ec were not able to follow to air temperature dynamics. Thus, Ec-n was estimated to be reliable for exact analysis of humidity dynamics under rapid change in air temperature, such as the vapor flux analysis, and for accurate control of air humidity.

INTRODUCTION

For measurement of air humidity in plant environments, many types of sensors are used (*2*, *3*, *6*). These sensors are made of different kinds of materials, and humidity is measured on the basis of different principles. Sensitivities or responses of these materials to air humidity are complicated with many factors, and it seems to bring various characteristics. For digital processing of data in time series (*1*, *4*, *7*, *8*), it is necessary to comprehend characteristics of the sensors, and to develop reliable instrumentation. Present paper deals with comparative analyses on static and dynamic characteristics in four typical types of humidity sensors.

TYPES OF HUMIDITY SENSORS

Four typical humidity sensors for air humidity measurement and control were used in this experiment, which were ventilated psychrometer of resistance thermometers (Ps; R220-10, CHINO WORKS, LTD.), lithium chloride relative humidity sensor (Lr; Q457A1019, Honeywell Inc.), electric capacitance meter (Ec; HMP15, Vaisala Oy) and absolute humidity sensor of thermistors (Ab; AH-1 SHIBAURA

Ps

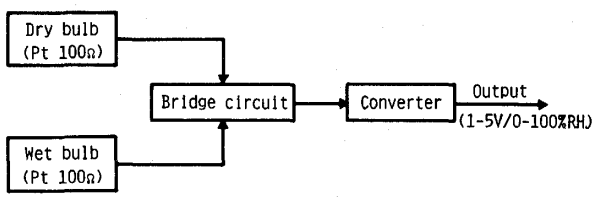
Dry bulb
(Pt 100Ω)
Bridge circuit
Converter
Output
(1-5V/0-100%RH)
Wet bulb
(Pt 100Ω)

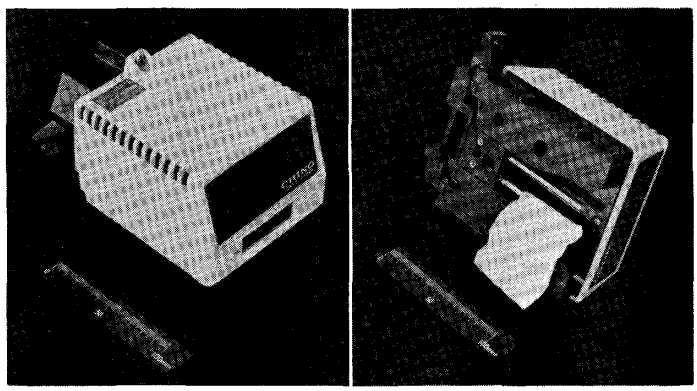

Lr

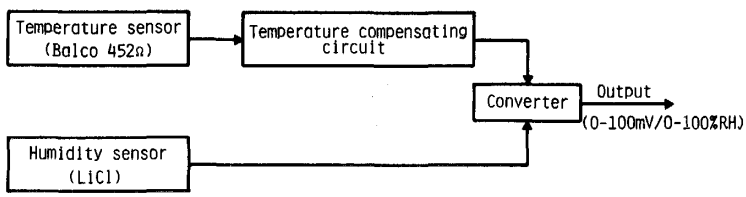
Temperature sensor
(Balco 452Ω)
Temperature compensating
circuit
Converter
Output
(0-100mV/0-100%RH)
Humidity sensor
(LiCl)

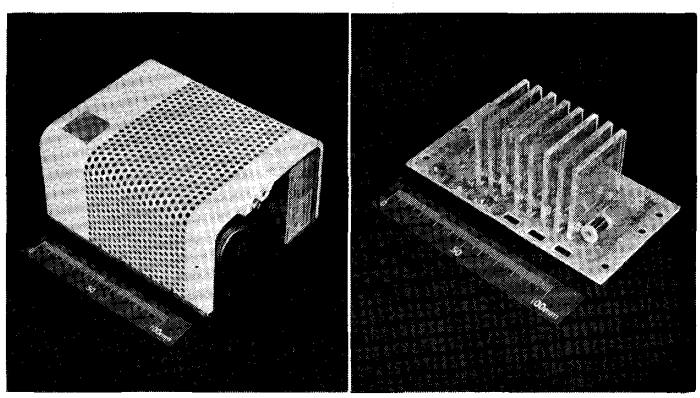

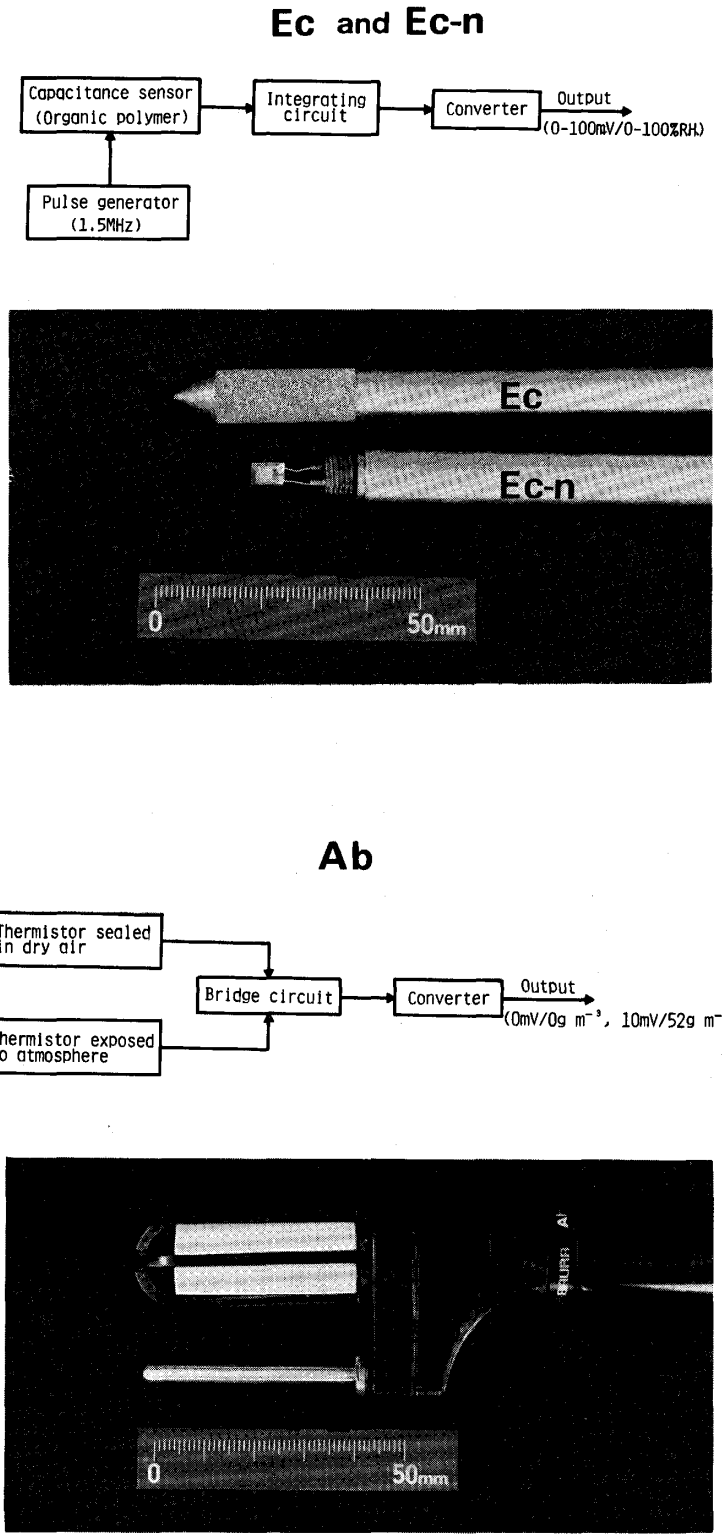

Fig. 1. System diagrams and photographs of ventilated psychrometer of resistance thermometers (Ps), lithium chloride relative humidity sensor (Lr), electric capacitance meter (Ec and Ec-n) and absolute humidity sensor of thermistors (Ab).

ELECTRONICS CO., LTD.). Block diagrams and photographs of respective sensors are shown in Fig. 1.

Ventilated psychrometer of resistance thermometers (Ps)

A pair of resistance thermometers (Pt100Ω) sheathed with insulating material in stainless steel tubes are equipped in a shelter with a water reservoir for wet-bulb. The shelter is ventilated by a fan at a constant air velocity of about 3 m sec^{-1}. One of the thermometers is a dry-bulb, and the other is a wet-bulb covered with wick of fourfold gauze (about 0.8 mm mesh). Output signal to relative humidity (RH) is obtained from difference between dry- and wet-bulb temperatures as 1–5V/0–100%RH through the bridge circuits and the converter. The operating humidity region distributes from 20 to 100% RH in an air temperature region of 5 to 60°C.

Lithium chloride relative humidity sensor (Lr)

Lr is composed of eight sensor elements consisting of two intermeshed gold electrodes mounted on a plastic plate ($38 \times 44 \times 3$ mm) and coated with a lithium chloride film. The lithium chloride contents in the films of respective elements are different in proportion to measuring ranges of humidity. Humidity is detected through changes in resistance of the element; the resistance varies with absorption or release of water vapour in the film. On the other hand, resistance of the element is also affected by air temperature. So, the temperature effect is compensated in the circuit with a thermometer (Balco 452Ω) built in the system. Thus, output signal of 0–100 mV/0–100%RH is obtained through the temperature compensating circuit and the converter. The operating humidity region distributes from 15 to 95%RH in an air temperature region of 5 to 50°C. Sensor elements are covered with a perforated protector for physical damage.

Electric capacitance meter (Ec, Ec-n)

Humidity is detected through change in electric capacitance of organic polymer dielectric; the electric capacitance varies with absorption and release of water vapour in the polymer. The sensor element is a thin film capacitor consisting of a glass plate (about $4 \times 6 \times 0.2$ mm), lower and upper gold electrodes and an organic polymer layer (about 1 μm in thickness); the organic polymer layer is sandwiched between upper and lower electrodes on the glass plate. This sensor element is built in the circuit of pulse oscillator in which pulse frequency varies around 1.5 MHz with capacitance of the element according to humidity change. Output signal of 0–100 mV/0–100%RH is obtained through the integrating circuit and the converter. The operating humidity region distributes from 0 to 100%RH in an air temperature region of −20 to 60°C. This small sized element is covered with a filter of gun metal (about 37 μm mesh) for protection from physical or chemical damages. In this experiment, two kinds of the system of capacitance meter are used; one (Ec) is a sensor with the gun metal filter and the other (Ec-n) is a sensor without the filter.

Absolute humidity sensor of thermistors (Ab)

The principle of Ab is based on the fact that thermal conductivity of air varies

with absolute humidity. A pair of bead thermistors (0.4 mm in diameter) is used in the system. One of the thermistors is a temperature compensating element which is sealed with dry air in a cylindrical metal case (4 mm in diameter, 7.5 mm in height), and the other is a humidity sensing element which is mounted in a metal case with four small vents perforated to be exposed to the atmosphere. These thermistors built in a bridge circuit are heated to about 200°C with Joul heat of their own current. The balance in this circuit is adjusted by using the sensor being exposed to dry air as a reference. When the sensor is exposed to moistened atmosphere, it generates unbalanced voltage caused by change in difference in resistance between two thermistors for temperature compensating and for humidity sensing, as heat transferring from the humidity sensing thermistor to the atmosphere varies with thermal conductivities of air according to change in absolute humidity. Absolute humidity is obtained as output of 0 mV at absolute humidity of 0 g m^{-3} and 10 mV at 52 g m^{-3} through the converter. The operating humidity region distributes from 0 to 52 g m^{-3} in an air temperature region of 10 to 40°C (from 0 to 84%RH at 40°C). The element is covered with a porous polyethylene filter (about 20 μm mesh) to prevent influence of wind on heat transfer from thermistors to the atmosphere.

STATIC AND DYNAMIC CHARACTERISTICS

Static characteristics

Static characterictics of respective sensors were examined in a growth chamber (*1*) in seven ranges of 20 to 80%RH at constant air temperatures of 40 and 10°C. Means of the outputs of respective sensors, which were read for 10 min at an interval of 2 min, were compared with humidities obtained from dry- and wet-bulb temperatures of modified type of ventilated psychrometer (Ps-j) established by Japan Meteorological Agency (*9*). Figure 2 shows the relations between outputs of sensors and humidities measured by Ps-j at air temperatures of 40 and 10°C. In Lr, hysterisis of about 2% RH was found at 40°C and higher humidities. The hysterisis was very slight in Ps, Ec and Ec-n, but not found in Ab. Linearities of Ps and Ab were lower than those of other sensors, and Ec and Ec-n brought slightly lower output elevation at 10°C; especially in Ps, the drift appeared to some extent at 10°C. Thus, the characteristics were specific to each sensor, but generally it could be estimated that all sensors can be applied to humidity measurement with an accuracy of ± 3%RH on the basis of calibration.

Step responses

In many cases of humidity measurements in plant environment, humidity is evaluated as relative humidity. Needless to say, relative humidity varies with both absolute humidity and air temperature. So, it is necessary to examine the dynamic characteristics of the sensor responding to air temperature change as well as to absolute humidity change. Step responses of the sensors to absolute humidity and air temperature were analysed. Step inputs of humidity to the sensors were performed in the processes of rising (from 30% to 80%RH) and falling (from 80% to 30%RH) at constant air temperatures and constant air velocities by using a

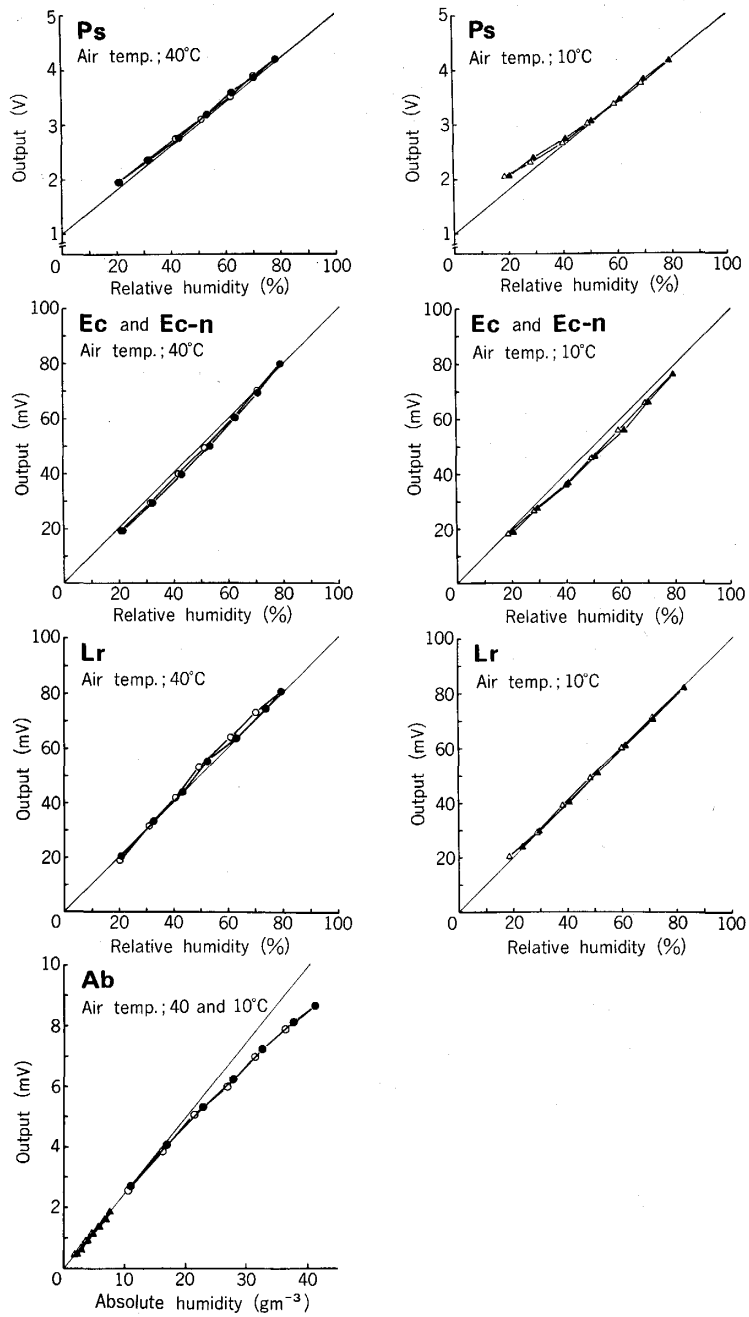

Fig. 2. Comparisons of outputs of sensors (Ps, Lr, Ec, Ec-n and Ab) with humidities obtained by psychrometer of Ps-j at air temperature of 40°C (●, humidity rising process; ○, humidity falling process) and 10°C (▲, humidity rising process; △, humidity falling process): Ps, ventilated psychrometer of resistance thermometers; Lr, lithium chloride relative humidity sensor; Ec, electric capacitance meter; Ec-n, electric capacitance meter (without filter); Ab, absolute humidity sensor of thermistors; Ps-j, modified type of ventilated psychrometer established by Japan Meteorological Agency.

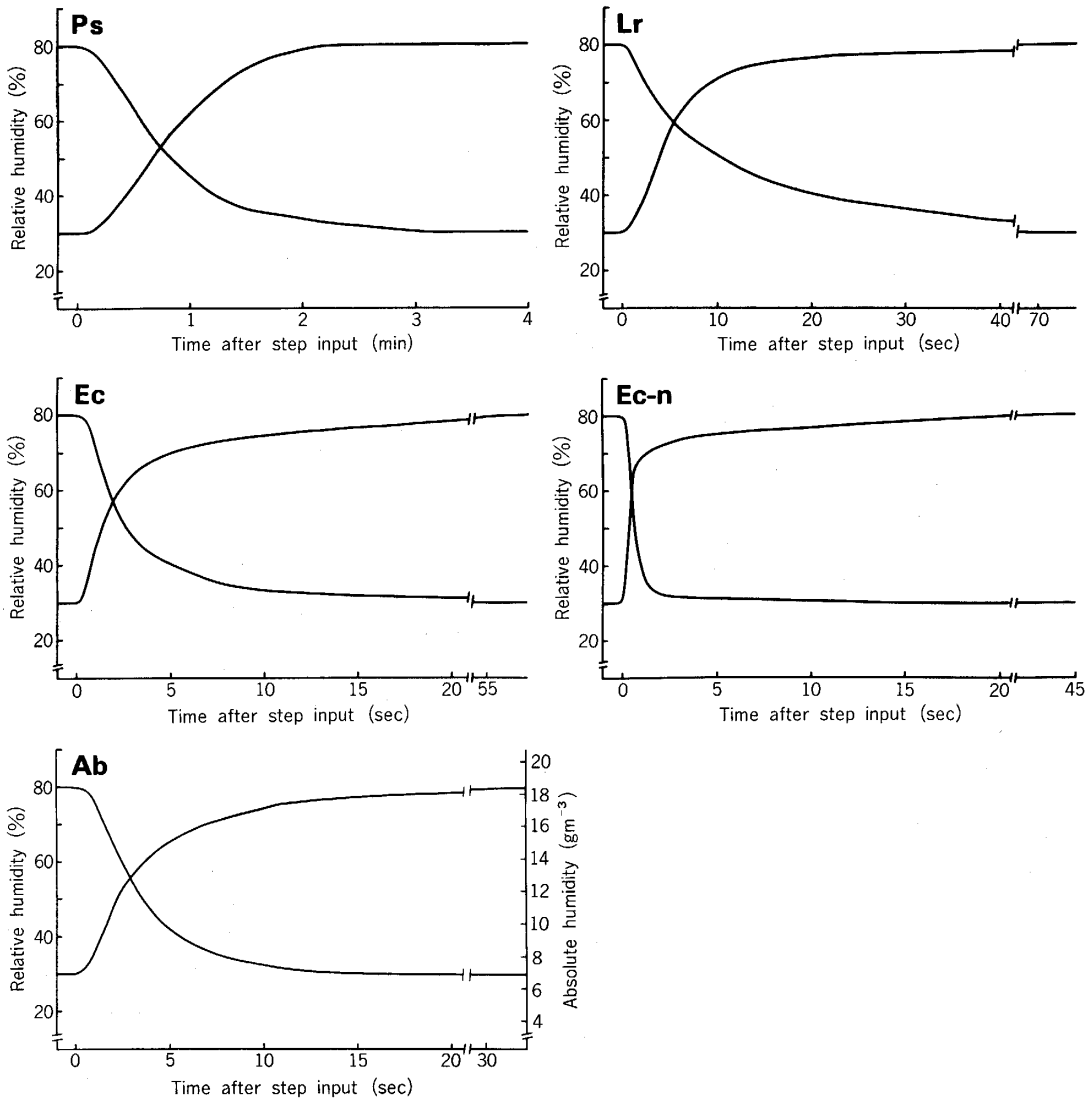

Fig. 3. Step responses of sensors (Ps, Lr, Ec, Ec-n and Ab) to humidity rising (from 30 to 80 %RH) and falling (from 80 to 30%RH) at air temperature of 25°C and air velocity of 0.6 m sec^{-1}: Ps, ventilated psychrometer of resistance thermometers; Lr, lithium chloride relative humidity sensor; Ec, electric capacitance meter; Ec-n, electric capacitance meter (without filter); Ab, absolute humidity sensor of thermistors.

plastic box (220×220×220 mm) in which step response of the sensor was examined; the sensor was set in the plastic box which was placed in the growth chamber and ventilated from an inlet to an outlet by a fan. The air controlled at an initial relative humidity was introduced into the plastic box, and the box was tightened for keeping the air in the box by shutting the inlet and the outlet. After the humidity in the growth chamber had been changed to the desired value of step input, the inlet and the outlet were opened and the air of growth chamber was introduced to the box rapidly by the ventilation. Thus, humidity in the box was changed within 0.5 sec in the step width of 30 to 80%RH or 80 to 30%RH. Sensors were exposed to this

Table 1. Delay times in step responses of sensors (Ps, Lr, Ec, Ec-n and Ab) to humidity rising (from 30 to 80% RH) and falling (from 80 to 30% RH) at air temperature of 25°C and air velocity of 0.6 m sec^{-1}: Ps, ventilated psychrometer of resistance thermometers; Lr, lithium chloride relative humidity sensor; Ec, electric capacitance meter; Ec-n, electric capacitance meter (without filter); Ab, absolute humidity sensor of thermistors.

Sensors	Delay time (sec)	
	Rising	Falling
Ps	47.0	41.0
Lr	4.6	7.2
Ec	1.7	2.2
Ec-n	0.5	0.6
Ab	5.6	6.0

rapid change in humidity for step response analyses. Air velocity in the box was controlled by setting rpm of the fan. In the case of analysis of Ps, water vapour evaporated from wet-bulb in the box was absorbed by using P_2O_5. Figure 3 shows humidity step responses of respective sensors at constant air temperature of 25°C and constant air velocity of 0.6 m sec^{-1}. In the step responses, there were not any overshoots, and the characteristics were examined by using the delay time which was defined as the time when the output reached to 50% of the desired value of step input. Delay times are listed in Table 1. Appreciable differences were found in delay time among the sensors. In Ps, delay time was remarkably longer than those of others, and dead time of about 4 sec was found. This fact indicates that the delay in Ps is brought by time lag of heat transfer in the wet-bulb of large heat capacity. Delay times in Lr and Ab were almost similar to each other. Ec and Ec-n showed more reliable responses as compared with those of others, but delay time in Ec became 3.5 times as long as that in Ec-n; the gun metal filter brought longer delay time in Ec. Furthermore, there were some differences in delay time between rising and falling processes, and this difference was distinct in Lr. This fact suggests that velocity of release of water vapour in Lr was lower than that of the absorption.

From the fact that higher air temperatures and higher air velocities increase the diffusivity of water vapour, it could be considered that step responses of the respective sensors to humidity are affected by air temperature and air velocity. Figure 4 shows step responses of respective sensors to humidity falling at respective air temperatures of 40, 25 and 10°C under constant air velocity of 0.6 m sec^{-1}. The effects of air temperatures on the delay times are shown in Fig. 5. Sensitivities of the sensors increased with higher air temperatures, and this temperature effect was different among the sensors. In particular, the effect of air temperature on delay time in Lr appeared larger than those in other sensors. From this fact, it could be conceivable that air temperature relates to the electrolysis of LiCl in Lr as well as to the diffusivity of water vapour. Figure 6 shows step responses of respective sensors to humidity falling at respective air velocities of 4.8, 2.4, 1.2, 0.6 and 0.3 m sec^{-1} under constant air temperature of 25°C. The effects of air velocities on the delay times are shown in Fig. 7. The delay times in Ec decreased in proportion to increase in air velocities.

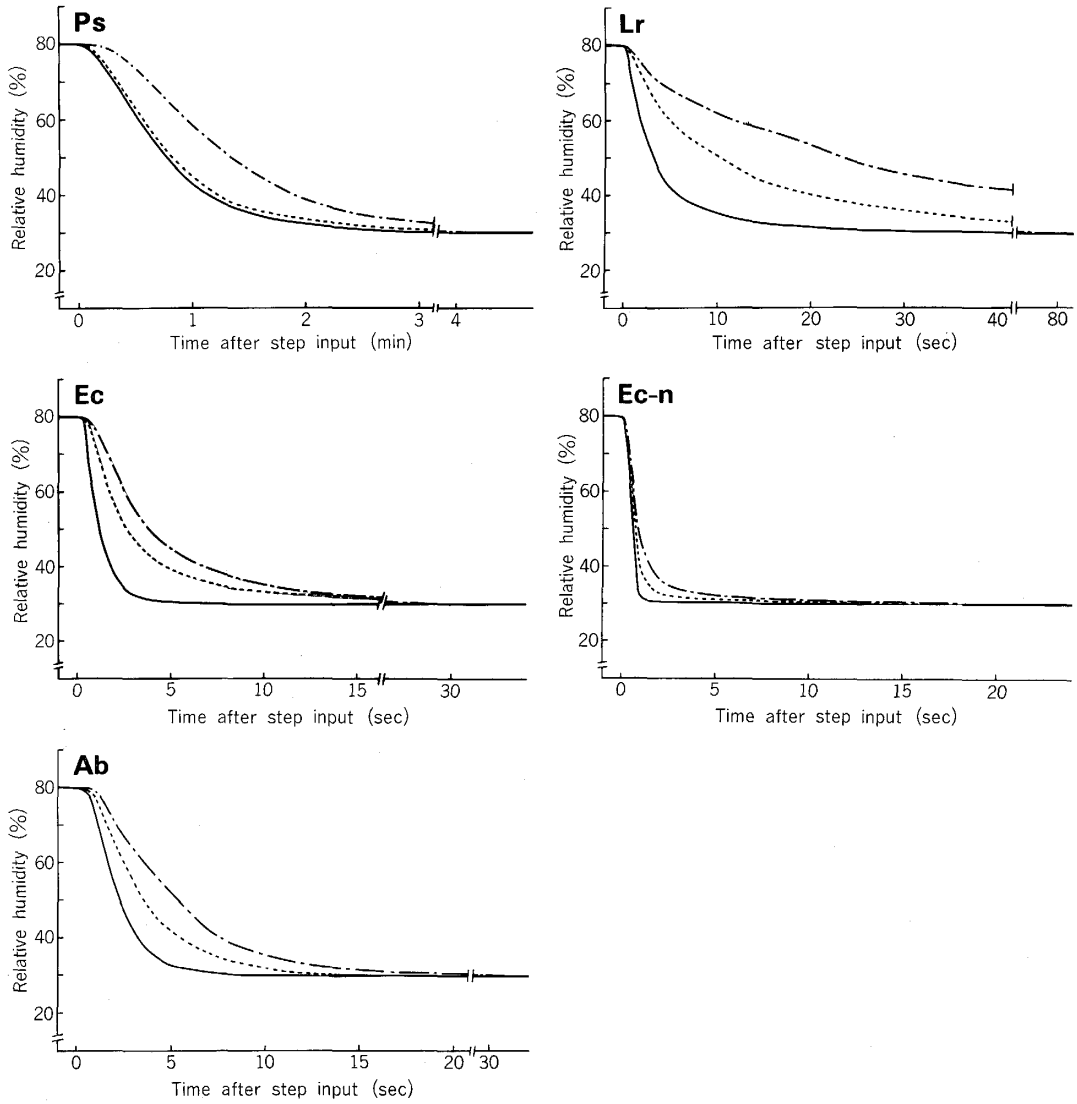

Fig. 4. Step responses of sensors (Ps, Lr, Ec, Ec-n and Ab) to humidity falling (from 80 to 30%RH) at respective air temperatures of 40 (——), 25 (- - -) and 10 (– – –)°C and air velocity of 0.6 m sec^{-1}: Ps, ventilated psychrometer of resistance thermometers; Lr, lithium chloride relative humidity sensor; Ec, electric capacitance meter; Ec-n, electric capacitance meter (without filter); Ab, absolute humidity sensor of thermistors.

In Lr, Ab and Ec-n, the delay times reduced rapidly in lower air velocities but became almost constant even in increased air velocities higher than 1.2 m sec^{-1}. On the other hand, air velocity scarcely affected the delay time in Ps; dry- and wet-bulb were always exposed to an air velocity of about 3 m sec^{-1} even if the air velocity (outside of the shelter) was changed, as the shelter covering Ps was ventilated constantly by a fan.

Step input of air temperature to the sensors was performed in a growth chamber (*5*) in the process of temp rature rising (from 20 to 30°C) at constant absolute

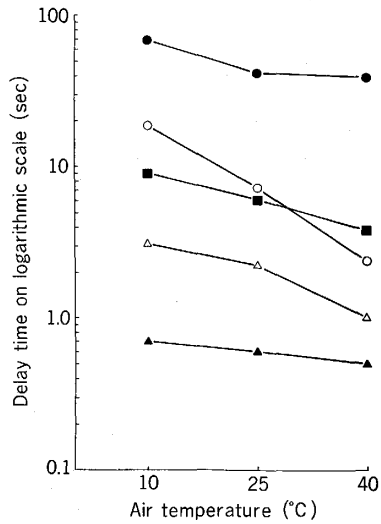

Fig. 5. Relations between air temperatures and delay times in step responses of sensors to humidity falling (from 80 to 30%RH) at air velocity of 0.6 m sec^{-1}: ●, ventilated psychrometer of resistance thermometers; ○, lithium chloride relative humidity sensor; △, electric capacitance meter; ▲, electric capacitance meter (without filter); ■, absolute humidity sensor of thermistors.

humidity of 14 g m^{-3} and constant air velocity of 0.6 m sec^{-1}. Air temperature in the growth chamber was changed within about 1 min in the step width of 20 to 30°C for the analyses of step responses. Air temperature in the growth chamber was measured by a copper-constantan thermocouple (0.1 mm in diameter) and dry-bulb of Ps, and at the same time, temperatures of the sensor element of Lr, of the filters of Ec and Ab, and of ambient air of Ec (inside of the filter) were also measured by the thermocouples. Figure 8 shows the sensor responses (a) and the respective temperatures (b). In the step response of Ec-n to air temperature, rising and settling times were shortest. The temperature step response of Ps appeared in similar pattern to that in the humidity step response stated above. On the other hand, the delay times of Ec and Lr became remarkably longer than those in humidity step responses; the delay times in temperature step responses of Ec and Lr were about 3 and 7 min, respectively, but the respective delay times in humidity step responses of those sensors were about 2 and 7 sec as shown in Table 1. Temperature rise in ambient air of Ec (inside of the filter) was affected by heat mass of the filter and delayed to some extent. This process resulted in longer delay time of Ec. In Lr, heat capacity of the sensor element is larger as compared with those in other sensors. This larger heat capacity in Lr brought longer delay time in temperature rise in the sensor element and resulted in lower rising rate of saturation deficit at the surface of the sensor element. Thus, the heat capacity of the sensor elements related to delay in the sensor responses to relative humidity change caused by step input of air temperature.

Furthermore, the sensors were exposed to both temperature and absolute humidity step inputs where temperature rapidly rose from 20 to 30°C, and at the same time absolute humidity fell from 14 to 11 g m^{-3} at constant air velocity of

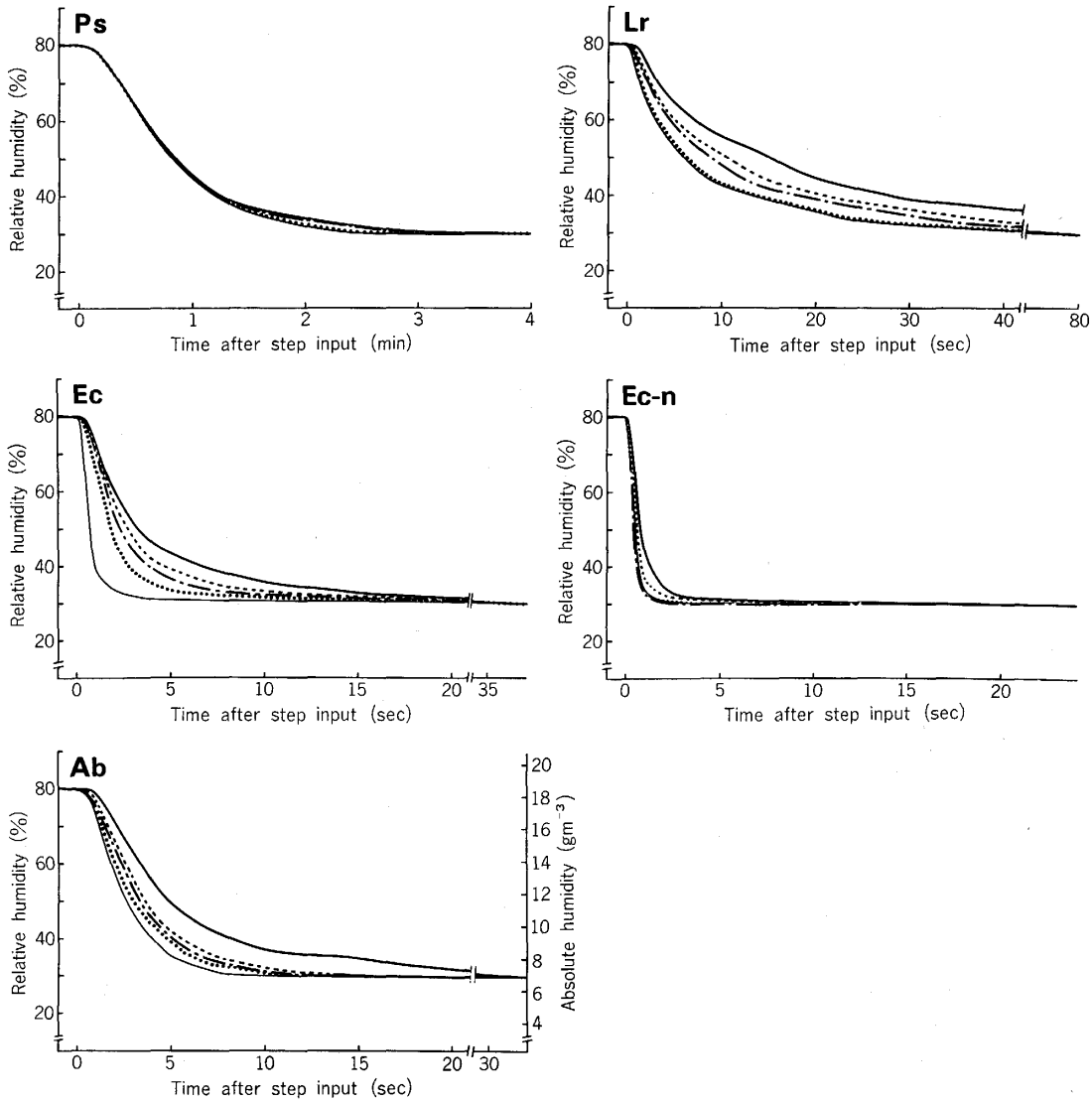

Fig. 6. Step responses of sensors (Ps, Lr, Ec, Ec-n and Ab) to humidity falling (from 80 to 30%RH) at respective air velocities of 4.8 (——), 2.4 (· · ·), 1.2 (– – –), 0.6 (- - -) and 0.3 (——) m sec^{-1} and air temperature of 25°C: Ps, ventilated psychrometer of resistance thermometers; Lr, lithium chloride relative humidity sensor; Ec, electric capacitance meter; Ec-n, electric capacitance meter (without filter); Ab, absolute humidity sensor of thermistors.

0.6 m sec^{-1}. Figure 9 shows the sensor responses (a) to both temperature and absolute humidity step inputs, and also shows respective temperatures (b) of air in the growth chamber, of the sensor element of Lr, of the filters of Ec and Ab, and of ambient air of Ec (inside of the filter). The responses of Ec and Lr to both temperature and absolute humidity step inputs appeared in shorter delay times as compared with those to only temperature step input shown in Fig. 8. The delay times in Ec-n and Ps were almost the same as those to only temperature step input. There was appreciable difference in pattern of the step responses between Ab and

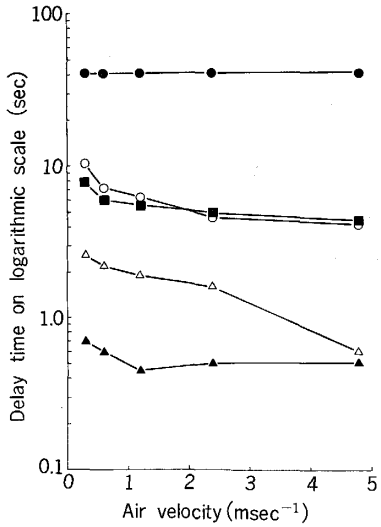

Fig. 7. Relations between air velocities and delay times in step responses of sensors to humidity falling (from 80 to 30%RH) at air temperature of 25°C: ●, ventilated psychrometer of resistance thermometers; ○, lithium chloride relative humidity sensor; △, electric capacitance meter; ▲, electric capacitance meter (without filter); ■, absolute humidity sensor of thermistors.

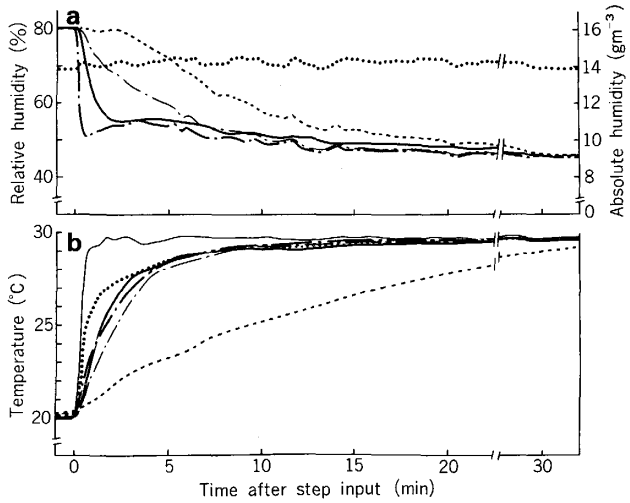

Fig. 8. Responses (a) of respective sensors of Ps (——), Lr (- - -), Ec (– – –), Ec-n (– – –) and Ab (· · ·) to air temperature step rising (from 20 to 30°C) at contant absolute humidity of 14 g m^{-3} and air velocity of 0.6 m sec^{-1}, and respective temperatures (b) of air in the growth chamber (——), of dry-bulb of Ps (——), of the sensor element of Lr (- - -), of the filters of Ec (– – –) and Ab (· · ·), and of air inside of the filter of Ec (– – –): Ps, ventilated psychrometer of resistance thermometers; Lr, lithium chloride relative humidity sensor; Ec, electric capacitance meter; Ec-n, electric capacitance meter (without filter); Ab, absolute humidity sensor of thermistors.

others. This difference could be considered to be caused by the delay in temperature compensation system of Ab. Temperature of the sensor element of Lr appeared in a unique pattern; the temperature fell 3°C just after the step inputs, and thereafter gradually rose. This fact indicated that change in heat which is caused by absorp-

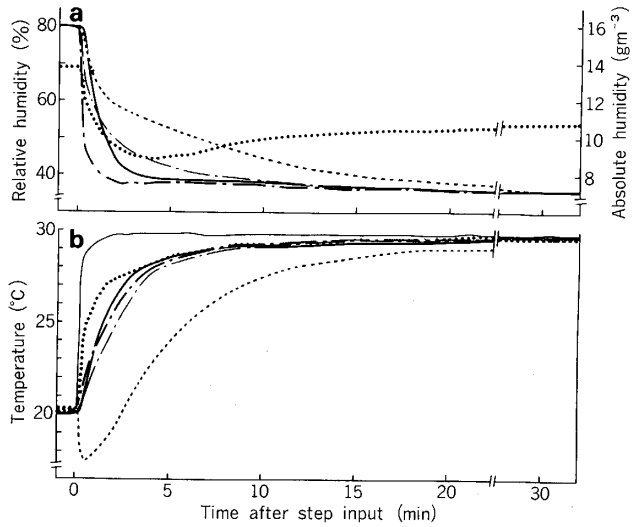

Fig. 9. Responses (a) of respective sensors of Ps (——), Lr (- - -), Ec (– – –), Ec-n (– – –) and Ab (· · ·) to both air temperature step rising (from 20 to 30°C) and absolute humidity step falling (from 14 to 11 g m^{-3}) at air velocity of 0.6 m sec^{-1}, and respective temperatures (b) of air in the growth chamber (——), of dry-bulb of Ps (——), of the sensor element of Lr (- - -), of the filters of Ec (– – –) and Ab (· · ·), and of air inside of the filter of Ec (– – –): Ps, ventilated psychrometer of resistance thermometers; Lr, lithium chloride relative humidity sensor; Ec, electric capacitance meter; Ec-n, electric capacitance meter (without filter); Ab, absolute humidity sensor of thermistors.

tion and release of water vapour in the sensor element of Lr relates to the temperature of the sensor element, and this event results in varying saturation deficit at the surface of sensor element.

Frequency responses

In most of the plant environments, air temperature and humidity fluctuate, and those fluctuations are complicated with different frequencies and amplitudes. For the practical use of the sensors, it is necessary to comprehend the frequency responses. So, the humidity sensors were exposed to simulated fluctuations of absolute humidity and air temperature; the frequency responses to sine wave inputs of absolute humidity and air temperature were analysed in the growth chamber (*5*) with use of Ec-n output as a reference, as Ec-n was most sensitive to air temperature and humidity dynamics as stated above.

Figure 10 shows the sensor responses (a) to sine wave input of absolute humidity with a period of 6 min and an amplitude of about 5 g m^{-3} at constant air temperature of 25°C and air velocity of 0.6 m sec^{-1}, and also shows respective temperatures (b) of air in the growth chamber, of the sensor element of Lr, of the filters of Ec and Ab, and of ambient air of Ec (inside of the filter). Phase lag and damped amplitude were clearly observed in Ps, but scarcely found in Lr, Ec and Ab; Lr, Ec and Ab responded well to the sine wave of absolute humidity, but Ps was not able to follow so reliably as the others.

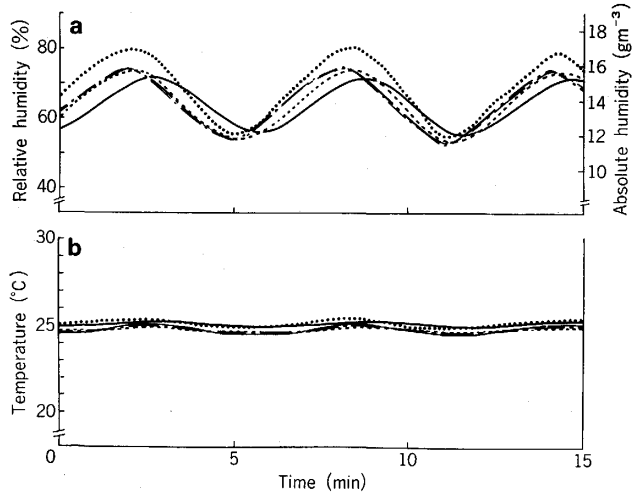

Fig. 10. Responses (a) of respective sensors of Ps (——), Lr (- - -), Ec (– – –), Ec-n (– – –) and Ab (· · ·) to sine wave (W_a=14 g m^{-3}±2.5 g m^{-3} sin 2πt/6; t, min) of absolute humidity (W_a) at constant air temperature of 25°C and air velocity of 0.6 m sec^{-1}, and respective temperatures (b) of air in the growth chamber (——), of dry-bulb of Ps (——), of the sensor element of Lr (- - -), of the filters of Ec (– – –) and Ab (· · ·), and of air inside of the filter of Ec (– – –): Ps, ventilated psychrometer of resistance thermometers; Lr, lithium chloride relative humidity sensor; Ec, electric capacitance meter; Ec-n, electric capacitance meter (without filter); Ab, absolute humidity sensor of thermistors.

Figure 11 shows the sensor responses (a) to sine wave input of air temperature with a period of 6 min and an amplitude of about 10°C at constant absolute humidity of about 14 g m^{-3} and constant air velocity of 0.6 m sec^{-1}, and also shows respective temperatures (b) of air in the growth chamber, of the sensor element of Lr, of the filters of Ec and Ab, and of ambient air of Ec (inside of the filter). Phase difference appeared at 180° between the output of Ec-n and the air temperature measured by the thermocouple in the growth chamber. This fact indicates that Ec-n responds exactly to change in relative humidity which is affected by the sine wave input of air temperature. Phase difference between output of Ps and the dry-bulb temperature was 180°, and phase lag and damped amplitude appeared almost the same as those in the sine wave input of absolute humidity. In Ec, phase lag and damped amplitude in the sine wave input of air temperature appeared more larger than those in the sine wave input of absolute humidity. Phase difference between output of Ec and the ambient air temperature of Ec (inside of the filter) was 180°. On the other hand, the output of Lr and the temperature of the sensor element were almost constant. From this fact, it could be estimated that Lr is not able to follow to the sine wave input of air temperature, because of the larger heat capacity of the sensor element.

The sensors were exposed to sine wave inputs of both absolute humidity and air temperature. Figure 12 shows the sensor responses (a) to the sine wave inputs of both absolute humidity and air temperature with a period of 6 min at air velocity of 0.6 m sec^{-1}, and also shows respective temperatures (b) of air in the growth chamber,

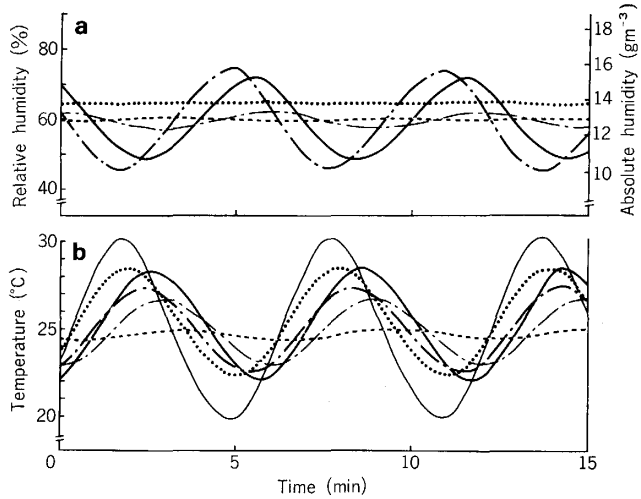

Fig. 11. Responses (a) of respective sensors of Ps (——), Lr (- - -), Ec (– – –), Ec-n (– – –) and Ab (· · ·) to sine wave (T_a=25°C±5°C sin 2πt/6; t, min) of air temperature (T_a) at constant absolute humidity of 14 g m^{-3} and air velocity of 0.6 m sec^{-1}, and respective temperatures (b) of air in the growth chamber (——), of dry-blub of Ps (——), of the sensor element of Lr (- - -), of the filters of Ec (– – –) and Ab (· · ·), and of air inside of the filter of Ec (– – –): Ps, ventilated psychrometer of resistance thermometers; Lr, lithium chloride relative humidity sensor; Ec, electric capacitance meter; Ec-n, electric capacitance meter (without filter); Ab, absolute humidity sensor of thermistors.

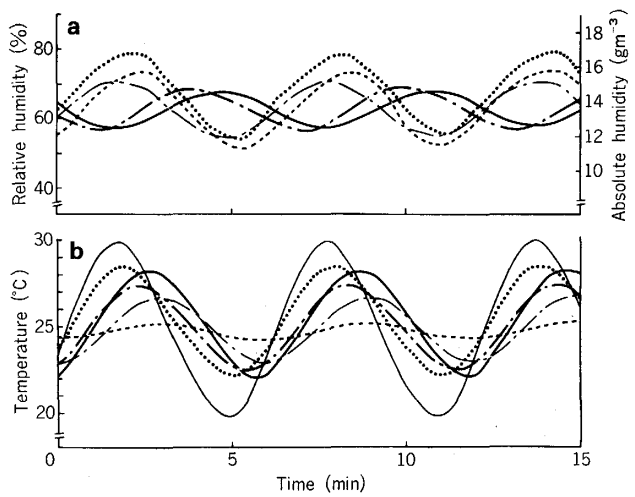

Fig. 12. Responses (a) of respective sensors of Ps (——), Lr (- - -), Ec (– – –), Ec-n (– – –) and Ab (· · ·) to sine waves of both absolute humidity (W_a=14 g m^{-3}± 2.5 g m^{-3} sin 2πt/6; t, min) and air temperature (T_a=25°C±5°C sin 2πt/6; t, min) at air velocity of 0.6 m sec^{-1}, and respective temperatures (b) of air in the growth chamber (——), of dry-bulb of Ps (——), of the sensor element of Lr (- - -), of the filters of Ec (– – –) and Ab (· · ·), and of air inside of the filter of Ec (– – –): Ps, ventilated psychrometer of resistance thermometers; Lr, lithium chloride relative humidity sensor; Ec, electric capacitance meter; Ec-n, electric capacitance meter (without filter); Ab, absolute humidity sensor of thermistors.

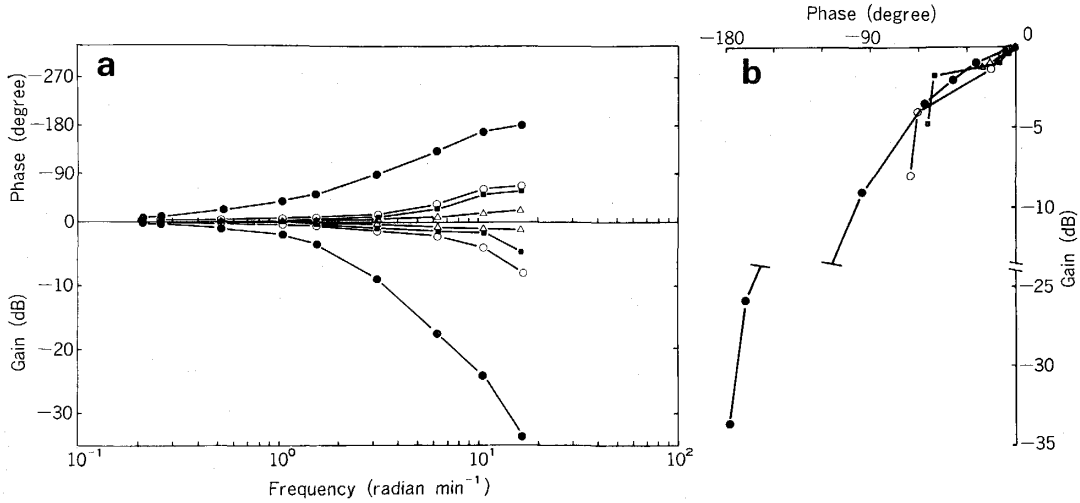

Fig. 13. Frequency responses (a, Bode diagram; b, gain-phase diagram) of sensors to absolute humidity fluctuation at constant air temperature of 25°C and air velocity of 0.6 m sec^{-1}: ●, ventilated psychrometer of resistance thermometers; ○, lithium chloride relative humidity sensor; △, electric capacitance meter; ■, absolute humidity sensor of thermistors.

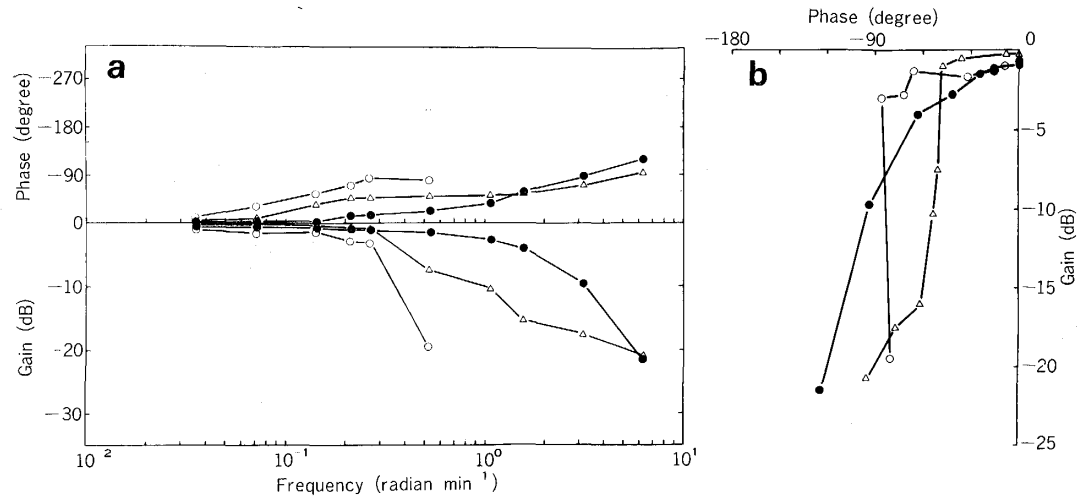

Fig. 14. Frequency responses (a, Bode diagram; b, gain-phase diagram) of sensors to air temperature fluctuation at constant absolute humidity of 14 g m^{-3} and air velocity of 0.6 m sec^{-1}: ●, ventilated psychrometers of resistance thermometers; ○, lithium chloride relative humidity sensor; △, electric capacitance meter.

of the sensor element of Lr, of the filters of Ec and Ab, and of ambient air of Ec (inside of the filter). The pattern of Ec-n output appeared different from those of Lr, Ec and Ab outputs. From the fact that the phase of Lr was similar to that of Ab, it could be conceivable that Lr responds reliably to the absolute humidity, but not so sensitive to air temperature fluctuation. The output of Ec was the same value as that of Ec-n at the time when the ambient air temperature of Ec (inside of the filter) became equal to the air temperature in the growth chamber. Thus, Ec responded

well to the sine wave input of absolute humidity and to change in ambient air temperature of Ec (inside of the filter), but was not able to follow to the sine wave input of air temperature in the growth chamber. In Ps, slight phase lag and damped amplitude were found. In all sensors, respective characteristics were similar to those found in Figs. 10 and 11. So, frequency responses to absolute humidity and air temperature were examined. In sensor responses to sine wave inputs of absolute humidity and air temperature with different frequencies, phase lags and gains were compared with Ec-n output. Figures 13 and 14 show frequency responses to absolute humidity and air temperature respectively, in Bode diagram (a) and in gain-phase diagram (b). In the frequency response to absolute humidity (Fig. 13), the characteristics of Ps was clearly different from those of others, but appreciable differences among the characteristics of Lr, Ec and Ab were not found in the frequence range used in this experiment. In the frequency response to air temperature (Fig. 14), characteristics of Ps, Lr and Ec were different from each other. For evaluation of the fidelity to the fluctuating input, the band width defined as the frequency at the point where the gain is $2^{-0.5}$ (about -3 dB) is used. The band widths to absolute humidity fluctuation were about 1.6 rad min^{-1} (period; $2\pi/\omega=$ 4 min) in Ps and higher than 9 rad min^{-1} (period; $2\pi/\omega=0.7$ min) in Lr, Ec and Ab. On the other hand, the band widths to air temperature fluctuation were 1.4 rad min^{-1} (period; $2\pi/\omega=4.5$ min) in Ps and lower than 0.35 rad min^{-1} (period; $2\pi/\omega=18$ min) in Lr and Ec. Thus, the difference between the frequency responses to absolute humidity and to air temperature was clearly found in Lr and Ec, but scarcely found in Ps. This fact indicates that the dominant lag factors in responses of Lr and Ec to air temperature fluctuation are different from those to absolute humidity fluctuation, but the dominant lag factor in Ps response to air temperature fluctuation is the same as that to absolute humidity fluctuation.

CONCLUSION

In static characteristics, all sensors could be estimated to measure humidity with an accuracy of $\pm 3\%$RH in steady state on the bases of respective calibrations within the operating humidity region. On the other hand, dynamic characteristics of the sensor responses to absolute humidity and air temperature changes were specific to each other, which were affected by air temperature, air velocity, filter effects and heat capacity of the sensor element. It is necessary that relative humidity sensor responds sensitively to air temperature dynamics as well as absolute humidity dynamics. In this experiment, Ec-n responded most sensitively to both absolute humidity and air temperature dynamics, but Ps, Lr, Ec and Ab were not necessarily sensitive to absolute humidity dynamics and/or air temperature dynamics. In particular, Lr and Ec were not able to follow to air temperature dynamics, although they were sensitive to absolute humidity dynamics. Thus, from the results of analyses of the dynamic characteristics, it could be estimated that Ec-n is the most reliable for exact analysis of humidity dynamics such as vapour flux analysis (*4*) and for accurate control of air humidity (*1*).

REFERENCES

1. Eguchi H., Kitano M. and Matsui T. (1984) Direct digital control of air humidity for plant research. *Biotronics* **13**, 29–38.
2. Forrester J. S. (1979) Humidity: Critique II. Pages 177–192 *in* T. W. Tibbitts and T. T. Kozlowski (eds) *Controlled Environment Guidelines for Plant Research*. Academic Press, New York.
3. Hall C. W. (1965) Problems of humidity and moisture in agriculture. Pages 87–94 *in* E. J. Amdur (ed) *Humidity and Moisture. Measurement and Control in Science and Industry*. Vol. 2. *Applications*. Reinhold Publishing Corp., New York.
4. Kitano M., Eguchi H. and Matsui T. (1983) Analysis of heat balance of leaf with reference to stomatal responses to environmental factors. *Biotronics* **12**, 19–27.
5. Matsui T., Eguchi H., Hanami Y., Handa S. and Terajima T. (1971) A growth cabinet for the study on biotronics. I. Design and performance. *Environ. Control in Biol.* **9**, 37–46.
6. Rosenberg N. J. (1974) Atmospheric humidity. Pages 128–144 *in Microclimate: The Biological Environment*. John Wiley & Sons, New York.
7. Takeuchi K., Ohtaki E. and Seo T. (1980) Turbulent transfer of water vapor over paddy fields. *Ber. Ohara Inst. Landwirtsch. Biol. Okayama Univ.* **18**, 1–30.
8. Tsukamoto O. and Mitsuta Y. (1982) Direct measurements of water vapor fluxes with different hygrometers. *Bull. Disaster Prevention Res. Inst., Kyoto Univ.* **25**, 283–295.
9. Yoshitake M. and Shimizu I. (1965) Experiment results of the psychrometer constant. Pages 70–75 *in* R. E. Ruskin (ed) *Humidity and Moisture. Measurement and Control in Science and Industry*. Vol. 1. *Principles and Methods of Measuring Humidity in Gases*. Reinhold Publishing Corp., New York.